

05,07

The magnetic phase of $CxGyFz$ in $HoFe_{1-x}Mn_xO_3$ single crystals at concentrations of manganese $x \leq 0.1$

© K.A. Shaykhutdinov, A.L. Freidman, S.A. Skorobogatov

Kirensky Institute of Physics, Federal Research Center KSC SB, Russian Academy of Sciences, Krasnoyarsk, Russia

E-mail: smp@iph.krasn.ru

Received November 20, 2024

Revised November 23, 2024

Accepted November 24, 2024

A detailed study of the magnetic and dilatometric properties of a series of $HoFe_{1-x}Mn_xO_3$ single crystals at low concentrations of manganese ($x = 0, 0.05, 0.1$) was carried out to refine the magnetic phase diagram in the region of low concentrations of manganese. From the results of measurements of magnetization and relative deformation carried out on a series of $HoFe_{1-x}Mn_xO_3$ single crystals, a new low-temperature magnetic phase $CxGyFz$ (for the space group of $Pnma$) was discovered, characterized by the direction of a weak ferromagnetic moment along the c axis of the crystal, which had not been previously observed. Thus, as the temperature decreases for concentrations $x = 0.05$ and 0.1 , a more complex transition of the spin reorientation $AxFyGz \rightarrow GxCyAz \rightarrow CxGyFz$ in $HoFe_{1-x}Mn_xO_3$ is observed, in contrast to the transition $AxFyGz \rightarrow GxCyAz$ realized in single crystals $HoFe_{1-x}Mn_xO_3$ with $x > 0.1$.

Keywords: orthoferrites, spin reorientation transition, magnetic phase diagram.

DOI: 10.61011/PSS.2024.12.60215.312

1. Introduction

Rare-earth orthoferrites with general formula $RFeO_3$ are an interesting family of rhombic crystals (space group № 62) from the point of view of their magnetic properties. They have a low ferromagnetic torque caused by chamfer of antiferromagnetic sublattices, which is explained by antisymmetric Dzyaloshinski–Moriya interaction [1,2]. They contain multiple defects, such as spontaneous spin-orientation transition [3–5], superfast remagnetization of antiferromagnetic domain walls when exposed to femtosecond laser impulses [6,7], observation of nontrivial spin dynamics in the rare-earth subsystem [8] etc. Many of these defects have a significant potential of practical use. Undoubtedly, the most extensively studied phenomenon of the above observed in orthoferrites is a spontaneous spin-reorientation transition, which was found and thoroughly investigated more than half a century ago. The temperature of this transition varies in a wide temperature range — from units of Kelvin degrees for $YbFeO_3$ [8] to 450 K for $SmFeO_3$ [9] and is determined by weak interaction between the subsystems of iron and rare earth. To change the temperature of spin-orientation transition T_{SR} , often isovalent substitution is used in the subsystem of iron [5,10–12], when the spin-reorientation transition may be observed both at nitrogen and room temperatures.

In our recent paper dedicated to the growth and research of a series of single crystals $HoFe_{1-x}Mn_xO_3$ ($0 < x < 1$) [13], it was shown that whenever the iron was substituted for manganese, the temperature of the spin-orientation transition increases substantially. Thus, at manganese concentration $x = 0.4$, $T_{SR} = 294$ K, while for the non-substituted compound $HoFeO_3$ $T_{SR} = 58$ K. Besides,

such substitution changes the type of magnetic-orientation transition from transition of order II ($AxFyGz \rightarrow CxGyFz$) ($x = 0$), when the weak ferromagnetic torque rotates from direction b to direction c of the crystal as the temperature decreases, to transition of order I ($AxFyGz \rightarrow GxCyAz$) with the presence of the weak ferromagnetic torque only in direction b (for installation $Pnma$) in the area of high temperatures.

According to the classic papers by Holmes [14,15], dedicated to research of the effect of isovalent substitution in the subsystem of iron at magnetic properties of orthoferrites, there is a critical concentration x_c , which changes the type of the orientation transition from the simple reorientation of the torque from one crystallographic direction to another one (transition of order II) to the transition of order I. Besides, these papers developed a model that described the temperature dependence $T_{SR}(x)$, which is determined by the following expression:

$$T_{SR}(x) = (1/k) \lg(x/x_c), \quad (1)$$

where k — positive constant value, related to the fields of anisotropy of the second order in $b-a$, $b-c$, $c-a$ planes, x_c — characterizes the critical concentration, when a transition to the state of collinear antiferromagnetic (phase $GxCyAz$) takes place. The authors studied variation of the constant values of anisotropy of the second order, responsible for the temperature of spin-reorientation transition, as the concentration of cobalt varies in orthoferrites of erbium, holmium and dysprosium [15] and manganese in orthoferrite of yttrium [14], and it was found that $x_c \approx 0.1$. In our case, having the series of previously grown single crystals $HoFe_{1-x}Mn_xO_3$, it would be logical to do a similar study for holmium orthoferrite.

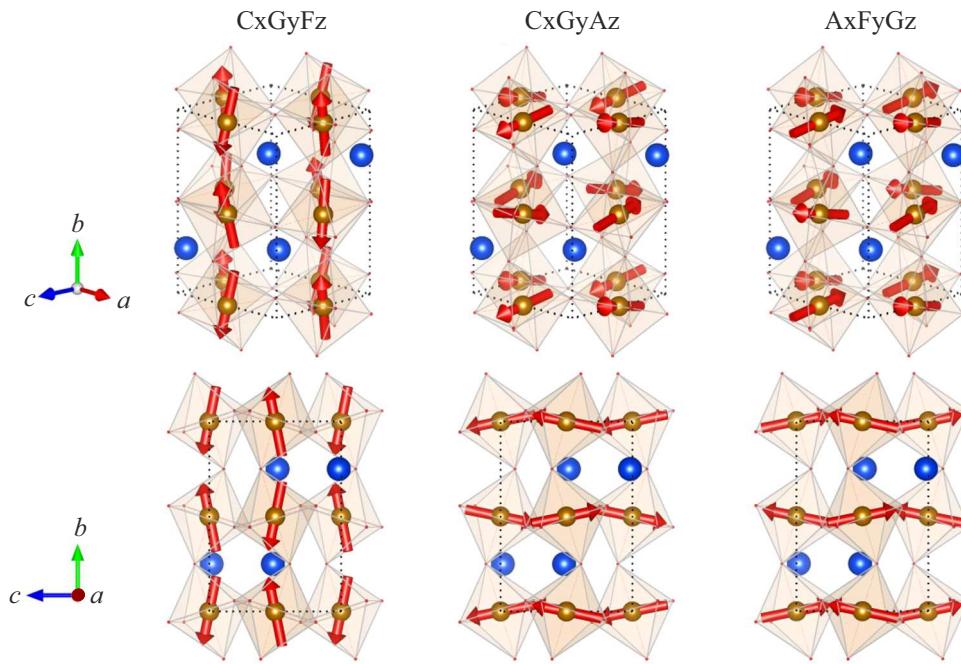


Figure 1. Layout view of magnetic structures implemented in single crystals $HoFe_{1-x}Mn_xO_3$.

Therefore, the purpose of this paper was detailed research of magnetic and dilatometric properties of a series of single crystals $HoFe_{1-x}Mn_xO_3$ at low concentrations of manganese ($x = 0, 0.05, 0.1$) to specify the magnetic phasing diagram in the region of critical concentrations x_c .

2. Experiment

Single crystals $HoFe_{1-x}Mn_xO_3$ ($x = 0, 0.05, 0.1$) were grown by the method of optical zone melting, the growth procedure, post-growth treatment and structural characterization are described in detail in paper [13]. All single crystals $HoFe_{1-x}Mn_xO_3$ are rhombic with the spatial symmetry group $Pnma$. In some papers of other authors an installation was used with the spatial symmetry group $Pbnm$, and the transition from one installation to another may be described as follows: $a, b, c (Pnma) \rightarrow b, c, a (Pbnm)$. To orient the produced specimens along the crystallographic axes, Laue diffractometer (Photonic Science) was used.

To measure the temperature and field dependences of magnetization for the grown single crystals in the temperature range 4.2–300 K, installation PPMS–6000 (Quantum Design) was used.

Measurement of the relative deformation of the specimens which occurred as a result of thermal expansion was determined using a manufactured capacitance dilatometer [16,17], adapted for operation within PPMS (Quantum Design). Measurements of relative deformation were carried out in the mode of free-running sweep of temperature with the speed of 0.25 K/min in the atmosphere of heat-exchange gaseous helium with residual pressure 4–6 mbar in the

temperature range from 4.2 to 200 K without application of the external magnetic field.

3. Results and discussion

3.1. Magnetic measurements

In the previous paper [13] it was shown that in a series of single crystals $HoFe_{1-x}Mn_xO_3$ at different concentrations of manganese x and temperatures T , magnetic phases $AxFyGz$, $CxGyFz$, $GxCyAz$ are implemented. They are schematically shown in Figure 1. It shows with arrows the directions of magnetic torques of iron (manganese) ions in a crystal, corresponding to the directions of a weak ferromagnetic torque along axes b and c , and also in the phase of the fully compensated antiferromagnetic.

Figure 2 shows temperature dependences of magnetization $M(T)$ for specimens with $x = 0.05$ (a) and 0.1 (b), measured along crystallographic directions b and c . Features on dependences $M(T)$ along direction b , observed at temperatures ~ 94 and ~ 141 K (black curves), are related to spin-reorientation transition (identified as SR1 in figure) and were observed by us previously when studying the magnetic properties of the entire series of single crystals $HoFe_{1-x}Mn_xO_3$ [13]. When cycling by temperature, these dependences show temperature hysteresis with width $\Delta T \approx 1$ K. Such temperature hysteresis is specific for phase transition of order I and complies with spin reorientation from phase $AxFyGz$ to the state of compensated antiferromagnetic $GxCyAz$. However, after the measurements of dependences $M(T)$ along direction c for single crystals with concentration of Mn $x = 0.05$ and 0.1 (red curves),

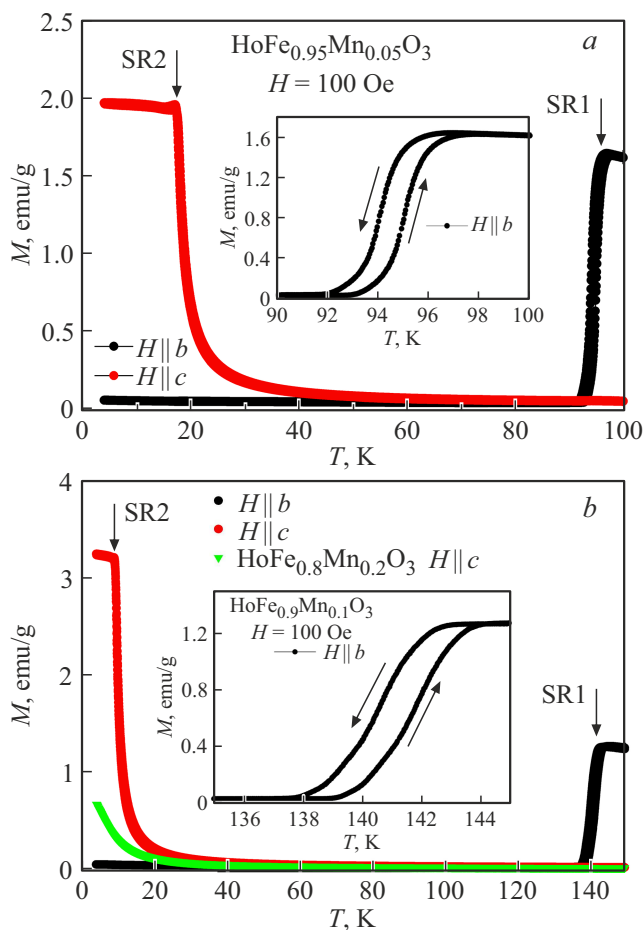


Figure 2. Temperature dependences of magnetization $M(T)$ for specimens with $x = 0.05$ (a) and 0.1 (b).

it turned out that in the region of low temperatures there is another spin-reorientation transition T_{SR2} at $T = 17$ K for $x = 0.05$ and $T = 9$ K for $x = 0.1$, directing the weak ferromagnetic torque along axis c of the crystal that was not observed previously. As the manganese concentration increases further, the orientation transition SR2 disappears. Thus, in Figure 2, b dependence $M(T)$ is shown along axis c for specimen $\text{HoFe}_{0.8}\text{Mn}_{0.2}\text{O}_3$ (green curve), where such feature is not observed up to helium temperatures, and increased value of magnetization in the region of low temperatures is related to paramagnetic contribution of holmium. It should also be noted that when cycling by temperature, no hysteresis feature was observed in the region of temperatures T_{SR2} , which means that the orientation transition SR2 relates to the phase transition of order II.

Therefore, at low concentrations of manganese $x = 0.05$ and $x = 0.1$ in $\text{HoFe}_{1-x}\text{Mn}_x\text{O}_3$ with temperature reduction the spin reorientation takes place in a more complicated way, as observed by us previously for solid solutions $\text{HoFe}_{1-x}\text{Mn}_x\text{O}_3$ with high concentrations. In the region of high temperatures the weak ferromagnetic torque is directed along axis b of the crystal (phase AxFyGz),

then at temperature T_{SR1} the magnetic torques of iron (manganese) are reoriented into the state of compensated antiferromagnetic (phase GxCyAz), and at temperature T_{SR2} phase CxGyFz is formed with ferromagnetic torque along axis c .

Figure 3 presents field dependences $M(H)$ for specimen $\text{HoFe}_{0.95}\text{Mn}_{0.05}\text{O}_3$ at different orientations of the applied external magnetic field. These dependences fully reflect all features of behavior of the temperature curves $M(T)$ (Figure 2). If field H is applied along axis b (Figure 3, a), weak ferromagnetic torque is only observed in the region of high temperatures. Below temperature T_{SR1} dependences $M(H)$ correspond to the state of collinear antiferromagnetic. As the field is applied along axis c of the crystal (Figure 3, b), the ferromagnetic state is observed only in the region of low temperatures, where one may see fast linear growth of magnetization values in the region of small magnetic fields (up to 3 kOe), then the magnetic torque increases gradually due to contribution of paramagnetic holmium (green curve). The same pattern is observed for a single crystal with $x = 0.1$.

Note that axis b is difficult for the rare-earth subsystem, which is seen from the comparison of dependences $M(H_b)$ and $M(H_c)$ at $T = 4.2$ K. In the field of 20 kOe the magnetic torque M_c reaches 60 emu/g, whereas M_b is about 10 emu/g in the same field and at the same temperature. Such behavior could have been explained by biasing with the field of 3d-subsystem. And indeed at temperature $T = 4.2$ K a weak ferromagnetic phase is implemented with a magnetic torque of 3d-subsystem, lying along axis c . Therefore, axis c is a preferred axis, and it is logical to expect a large magnetic response from the rare-earth subsystem along this direction. Actually, this is the behavior observed on dependence $M(H_c)$ at $T = 4.2$ K in Figure 3, b . As one may see from the chart, the magnetization curve obviously consists of two processes, one of which ends in field ~ 3 kOe, and the second one continues in the higher fields. We assume that rapid growth of magnetization in the field up to 3 kOe is related to the growth of magnetic domains, the magnetic torque of which matches the external magnetic field. The further growth of magnetization is related to paramagnetic ordering of the holmium subsystem. However, application of the field along axis a also causes significant growth of magnetic torque, in other words the plane ac is easy for the rare-earth subsystem. This follows from the measurements of single crystal HoFeO_3 we took in the region of helium temperatures. Therefore, the weak paramagnetic response of the holmium subsystem along direction b may not be fully explained by the presence of the weak ferromagnetic torque in the orthogonal direction, and is rather related to single-ion anisotropy.

Besides, the nature of field dependence $M(H_b)$ behavior at high temperatures also stands out. At $T = 300$ K the weak ferromagnetic phase is implemented directing the spontaneous magnetic torque along axis b . As one may see from Figure 3, a remagnetization in this phase is accompanied with pronounced hysteresis. Besides, we

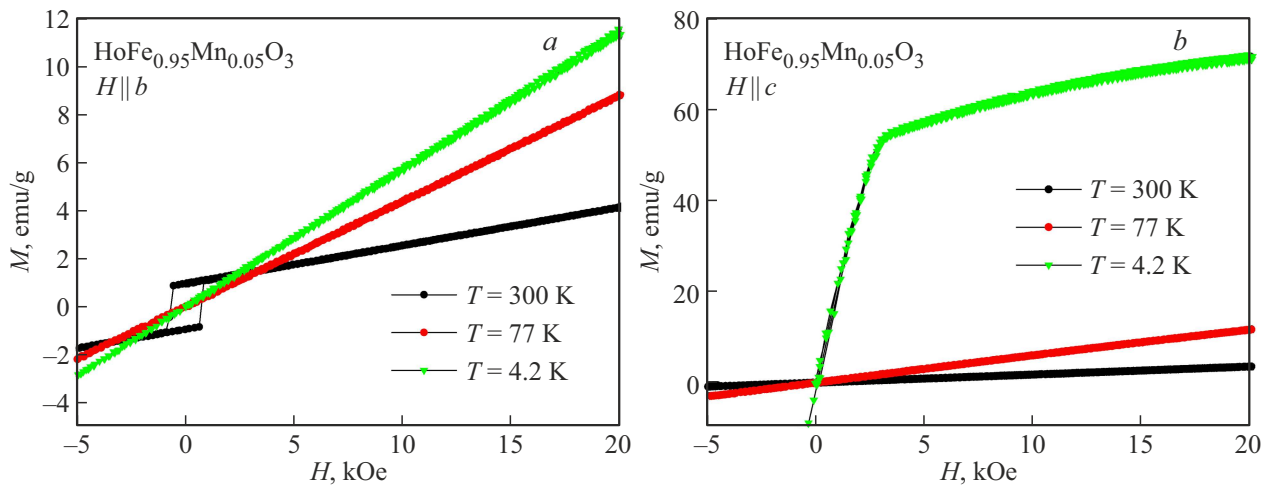


Figure 3. Field dependences $M(H)$ for specimen $HoFe_{0.95}Mn_{0.05}O_3$ at different orientations of the applied external magnetic field.

attempted to demagnetize a macroscopic single-crystal specimen in alternating magnetic field of decreasing amplitude at 300 K, however, we failed to break the specimen into magnetic domains. In general it should be concluded that the high temperature phase has higher coercive force than the low-temperature one.

This is related, first of all, to the fact that the phase with the weak ferromagnetic torque directed along axis b is implemented at high temperature, where the paramagnetic response from the rare-earth subsystem is weak. Second, direction b is difficult for the rare-earth subsystem as such.

In the low-temperature phase the rare-earth subsystem, on the contrary, contributes greatly to the magnetization process, since, first of all, the low-temperature susceptibility of the holmium subsystem is higher than that of the high-temperature one, and second, direction c is easy therefor. Since $4f$ -subsystem demonstrates paramagnetic behavior, for which the coercive force is equal to zero, and as a result of large contribution of the rare-earth subsystem into the magnetization process, no pronounced hysteresis is observed in the low-temperature phase in dependence $M(H)$, contrary to the high-temperature one.

3.2. Dilatometric measurements

Figure 4 shows dependences of relative deformation $\lambda(T)$ of a single crystal with $x = 0.05$, caused by thermal expansion (without application of the external magnetic field) along the three crystallographic directions a , b and c . The charts, as temperature rises, show two specific abnormalities at temperatures T_{SR2} and T_{SR1} , which consist in the jump of relative deformation, corresponding to spin-reorientation transitions $CxGyFz \rightarrow GxCyAz$ and $GxCyAz \rightarrow AxFyGz$, respectively.

As the temperature increases, relative deformation in point T_{SR2} experiences a jump, and along direction b the crystal expands, while along directions a and c it compresses. When temperature T_{SR1} is reached, the relative

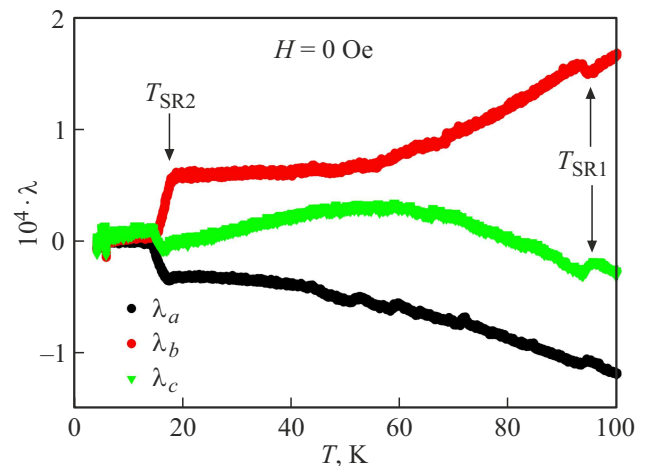


Figure 4. Relative deformation λ of single crystal $HoFe_{1-x}Mn_xO_3$, as function of temperature for three crystallographic directions a , b and c ($Pnma$), measured without application of the external magnetic field.

deformation along all three directions experiences a jump again, and now opposite in sign to the jump observed at T_{SR2} .

Such drastic change of thermal deformation at temperatures of transitions T_{SR2} and T_{SR1} is related to spontaneously occurring magnetostriction, which accompanies the readjustment of the magnetic structure. In high- and low-temperature states, when there is a weak ferromagnetic torque present, rare-earth ions are in molecular (magnetic) field of $3d$ -subsystem, which provides for the possibility of magnetostriction related to single-ion anisotropy of ion Ho^{3+} or exchange striction. In the intermediate temperature this factor is absent, and the spontaneous magnetic torque is zero. Therefore, subsequent transition over temperatures T_{SR2} and T_{SR1} is accompanied by connection and disconnection of spontaneous magnetic torque, which is related to the

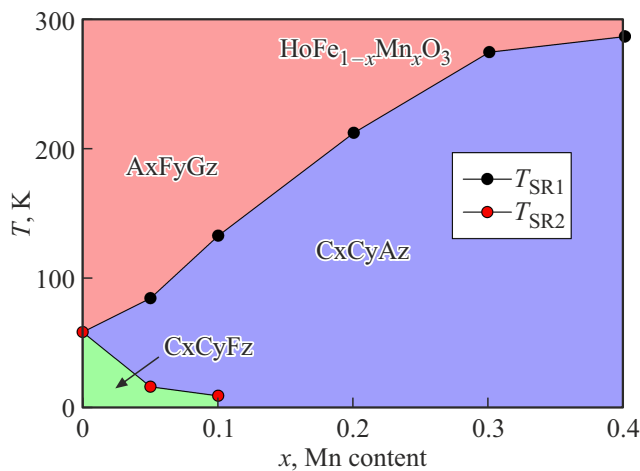


Figure 5. Magnetic phasing diagram $\text{HoFe}_{1-x}\text{Mn}_x\text{O}_3$.

mechanism of magnetostriction formation, which explains the different sign of deformation jump at temperatures T_{SR2} and T_{SR1} .

3.3. Magnetic phasing diagram $\text{HoFe}_{1-x}\text{Mn}_x\text{O}_3$

Using the results of measurements of magnetization and relative deformation done on a series of single crystals $\text{HoFe}_{1-x}\text{Mn}_x\text{O}_3$, one may conclude that we found a new low-temperature magnetic phase CxGyFz , characterized by direction of a weak ferromagnetic torque along axis c of the crystal, which was not observed previously. As temperature decreases for concentrations $x = 0.05$ and 0.1 , a more difficult transition of spin reorientation $\text{AxFeGz} \rightarrow \text{CxGyAz} \rightarrow \text{CxGyFz}$ is observed. Such behavior is illustrated in Figure 5, which represents a specified phasing diagram $\text{HoFe}_{1-x}\text{Mn}_x\text{O}_3$. Temperatures of spin-reorientation transition T_{SR1} for concentrations $x > 0.1$ are taken from paper [13]. Our data confirm that the critical concentration x_c lies in region $0.1 < x_c < 0.2$.

4. Conclusions

The key conclusion of the paper may be the detection of magnetic phase CxGyFz in a series of single crystals $\text{HoFe}_{1-x}\text{Mn}_x\text{O}_3$ in the region of small concentrations of manganese $x < 0.1$. At temperatures below orientation transition HoFeO_3 ($T = 58$ K) for substituted compositions $x < 0.1$ weak ferromagnetic state CxGyFz perseveres with a vector of a weak ferromagnetic torque directed along crystallographic axis c . It was found that phase transition SR1 is a phase transition of order I, while transition SR2 — transition of order II. In the region of these transitions, abnormalities of thermal expansion behavior were found, being related to spontaneous magnetostriction. In the temperature interval between SR1 and SR2 the intermediate collinear phase GxCyAz is implemented.

Funding

The study was supported by grant No. 23-22-10026 provided by the Russian Science Foundation, <https://rscf.ru/project/23-22-10026/>, Krasnoyarsk Regional Science Foundation.

Conflict of interest

The authors declare that they have no conflict of interest.

References

- [1] I.E. Dzyaloshinsky. J. Phys. Chem. Solids **4**, 241 (1958).
- [2] T. Moriya. Phys. Rev. **120**, 91 (1960).
- [3] R.L. White, J. Appl. Phys. **40**, 1061 (1969).
- [4] K.P. Belov, A.K. Zvezdin, A.M. Kadomtseva, I.B. Krynetsky. ZhETF **67**, 1974 (1975). (in Russian).
- [5] K. Belov, A. Zvezdin, A. Kadomtseva, R. Levitin. Orientatsionnye perekhody v redkozemelnykh magnetikakh, Nauka, Moscow (1979). (in Russian).
- [6] A.V. Kimel, A. Kirilyuk, P.A. Usachev, R.V. Pisarev, A.M. Balbashov, Th. Rasing. Nature **435**, 655 (2005).
- [7] J.A. de Jong, A.V. Kimel, R.V. Pisarev, A. Kirilyuk, Th. Rasing. Phys. Rev. B **84**, 104421 (2011).
- [8] S.E. Nikitin, L.S. Wu, A.S. Sefat, K.A. Shaykhutdinov, Z. Lu, S. Meng, E.V. Pomjakushina, K. Conder, G. Ehlers, M.D. Lumsden, A.I. Kolesnikov, S. Barilo, S.A. Guretskii, D.S. Inosov, A.B. Podlesnyak. Phys. Rev. B, **98**, 6, 064424 (2018).
- [9] J. Kang, Y. Yang, X. Qian, K. Xu, X. Cui, Y. Fang, V. Chandragiri, B. Kang, B. Chen, A. Stroppa, Sh. Cao, J. Zhang, W. Ren. IUCrJ, MATERIALS/COMPUTATION **4**, 598–603 (2017).
- [10] W. Fan, H. Chen, G. Zhao, X. Ma, R. Chakaravarthy, B. Kang, W. Lu, W. Ren, J. Zhang, Sh. Cao. Frontiers of Physics, **17**, 3, 33504 (2022).
- [11] L. Su, X.-Q. Zhang, Q.-Y. Dong, Y.-J. Ke, K.-Y. Hou, H.-T. Yang, Zh.-H. Cheng. Physica B: Cond. Mat. **575**, 411687 (2019).
- [12] Z. Sun, H. Song, S. Zhu, X. Ma, W. Yang, C. Shi, B. Kang, R. Jia, J.-K. Bao, S. Cao. J. Phys. Chem., **127**, 35, 17592 (2023).
- [13] K.A. Shaykhutdinov, S.A. Skorobogatov, Yu.V. Knyazev, T.N. Kamkova, A.D. Vasiliev, S.V. Semenov, M.S. Pavlovsky, A.A. Krasikov. ZhETF **165**, 5, 685 (2024). (in Russian).
- [14] L.M. Holmes, L.G. Van Uitert, R.R. Hecker. AIP Conf. Proc. **5**, 690 (1972).
- [15] L. Holmes, L. Van Uitert, R. Hecker. J. Appl. Phys. **42**, 657 (1971).
- [16] A.L. Freidman, S.I. Popkov, S.V. Semenov, P.P. Turchin. Pisma v ZhTF, **44**, 3, 79 (2018). (in Russian).
- [17] Patent na izobretenie № 2645823 „Emkostny dilatometr dlya raboty v sostave ustanovki PPMS QD“. A.L. Freidman, S.I. Popkov, N.V. Mikhashenok, S.G. Antonov (in Russian). Date of state registration in the State Register of Inventions of the Russian Federation February 28, 2018.

Translated by M.Verenikina